RESEARCH MEMORANDUM

BUFFETING FORCES ON TWO-DIMENSIONAL AIRFOILS AS

AFFECTED BY THICKNESS AND THICKNESS

DISTRIBUTION

By Charles F. Coe and Jack A. Mellenthin

Ames Aeronautical Laboratory
Moffett Field, Calif.

NATIONAL ADVISORY COMMITTEE
FOR AERONAUTICS

WASHINGTON
February 4, 1954

.H

NATIONAL ADVISORY COMMITTEE FOR AERONAUTICS

RESEARCH MEMORANDUM

BUFFETING FORCES ON TWO-DIMENSIONAL AIRFOILS AS

AFFECTED BY THICKNESS AND THICKNESS

DISTRIBUTION

By Charles F. Coe and Jack A. Mellenthin

SUMMARY

An experimental investigation has been conducted to determine the effect of thickness and of thickness distribution on the fluctuations of normal-force and pitching-moment coefficients of airfoils. Seven symmetrical airfoils were tested. Thickness was varied from 12 percent to 2 percent with 65A-series airfoils, while the thickness distribution was varied to give positions of maximum thickness from about 0.16 chord to about 0.63 chord for 8-percent-thick airfoils. A 4-percent-thick circular-arc airfoil was also tested. The test Mach number was varied from about 0.4 to 0.9, which corresponded to test Reynolds numbers from about 4.6 million to 8 million.

From the results there appeared to be two principal types of pressure pulsations associated with buffeting forces: pulsations which arise from intermittent build-up and dropping of the leading-edge pressure peak, and pulsations which are attributable to shock-wave motion and unsteady air flow following the shock wave.

No one of the seven airfoils tested had the lowest normal-force fluctuations over the entire range of Mach numbers and normal-force coefficients investigated. For Mach numbers below 0.6, fluctuation intensities were lowest on either the NACA 65A012 or NACA 2-008 airfoils but, for Mach numbers of 0.75 and above, the intensities were generally lowest on the NACA $65(06)A004$. Since the NACA $65(06)A002$ airfoil experienced higher intensities than the NACA $65(06)A004$, it appears that there may be a limit to the beneficial effects which a reduction of thickness has on buffeting forces. These results also indicate that an improvement might be made in the low-speed buffeting-force characteristics of the NACA $65(06)A004$ airfoil with only a small sacrifice in its superior characteristics at the higher speeds by moving the position of maximum thickness forward and by using a larger leading-edge radius than that of the $65(06)A004$ airfoil.

Fluctuations of pitching moment appeared small and would probably have little influence on the selection of an airfoil section for most purposes.

INTRODUCTION

Considerable research is now being undertaken in an effort to satisfy the need for a thorough coverage of the many parameters involved in the problem of buffeting. Investigations such as those contained in references 1 and 2 have established the existence of large pressure pulsations on rigid airfoils. It has been found that the characteristics of these pulsations vary with airfoil geometry. The purpose of this report is to consider types of pulsations which may be associated with buffeting, and also to present the normal-force and pitching-moment fluctuations which result from these pulsations as affected by airfoil-section geometry. Although the extent that these results for nearly rigid airfoils in two-dimensional flow apply to elastic three-dimensional wings is not known, it is believed that the trends shown reveal important factors affecting the buffeting of aircraft.

Seven two-dimensional airfoils were tested in this investigation in the Ames 16-foot high-speed wind tunnel. The airfoils were of various thicknesses and thickness distributions. The data were obtained at Mach numbers from about 0.4 to 0.9 with a corresponding Reynolds number range from about 4.6 million to 8 million.

NOTATION

c_n section normal-force coefficient

Δc_n one-half the average of the largest three peak-to-peak fluctuations of the section normal-force coefficient

Δc_m root mean square (rms) of the fluctuations of section pitching-moment coefficient from the mean

M free-stream Mach number

P pressure coefficient, $\dfrac{p - p_o}{q_o}$

P_{cr} critical pressure coefficient

p local static pressure

p_0 free-stream static pressure

q_0 free-stream dynamic pressure

APPARATUS AND INSTRUMENTATION

Wind Tunnel

The tests were conducted in a two-dimensional channel in the Ames 16-foot high-speed wind tunnel. Figure 1 is a photograph of the channel which was formed by two walls spaced 18.5 inches apart. The wall installation and pressure distributions along the walls were as described in reference 3.

Models

A sketch of the section profiles investigated is shown in figure 2. To investigate the effect of thickness, 65A-series airfoils having thickness ratios of 12, 8, 4, and 2 percent were selected.[1] To study the effects of variations of the chordwise distribution of thickness, two additional 8-percent-thick airfoils were chosen with positions of maximum thickness reasonably far ahead of and behind the 42-percent-chord position. For the former, an NACA 2-008 airfoil, which has received considerable attention due to its high-lift characteristics at low speeds, was chosen. Its maximum thickness is at about 16-percent chord. To obtain a rearward position of the maximum thickness (approximately 63-percent chord), an NACA 847A110 airfoil was modified to a symmetrical section by using the lower-surface coordinates given in reference 4 for both upper and lower surfaces and then reducing the thickness ratio to 8 percent. This airfoil will be designated in this report as the NACA 877A008. A 4-percent-thick circular-arc airfoil was also tested since it was felt that it would help indicate the effect that a sharp leading edge might have on buffeting forces.

The airfoils investigated had 2-foot chords and approximately 18-1/4-inch spans. The spaces between the models and the mounting walls were sealed with felt on one side and with a spring-loaded seal on the other. The models were of rigid construction. The 12-percent- and 8-percent-thick models were fabricated of wood with steel reinforcing, while the thinner models were aluminum.

---

[1]The ordinates of the 65A-series airfoils having thickness ratios of 4 and 2 percent were obtained by linearly scaling the ordinates for the 65A006 airfoil.

Instrumentation

A sketch of a typical model showing the arrangement of pressure cells and orifices, along with a table of their chordwise locations for each model, is given in figure 3. Each of the models, except the one having the NACA $65_{(06)}A002$ section, was provided with 30 flush-diaphragm-type electrical pressure cells near its midspan. Fifteen cells were located on the upper surface and fifteen on the lower surface of each airfoil. Due to the thinness of the 2-percent model, only 18 cells were installed.

The basic electronic apparatus and pressure cells used are described in reference 5. For this investigation the upper- and lower-surface cells at each station were mounted in matched pairs and connected electrically so that only the differences in pressure were recorded. Due to the thinness of the models, the corresponding cells on the upper and lower surfaces were staggered five-eights inch toward opposite sides of the model midspan to allow clearance for the backs of the cells. In addition, an integrating circuit was incorporated in the system so that a simultaneous indication proportional to instantaneous normal force could be recorded.

From an orifice adjacent to each cell, tubing was brought out of the model to the test equipment and then returned to the model and connected to the back of the pressure cell. At the test equipment, switches were incorporated in the circuit with connections which allowed either measurement of the static pressure or calibration of the cells. Approximately 50 feet of tubing was required to complete the circuit, which was more than enough to assure that any pulsations in local reference pressure were completely damped out.

The electrical responses from each pair of pressure cells and from the summing circuit were recorded on oscillographs. The galvanometer elements used in these oscillographs have an amplitude response which is flat to about 60 cycles per second and then drops to about 50 percent of that amplitude at 170 cps. Although the frequency response of these elements is rather limited, it was found that the intensities obtained were within 10 percent of those obtained from duplicate tests using elements having a flat response to approximately 500 cps. Since the traces from the higher-frequency elements contained a considerable amount of high-frequency background noise, the lower-frequency elements were used in order to facilitate analysis of the data.

PROCEDURE

Range of Test Variables

The investigation was conducted over a Mach number range from about 0.4 to 0.9. The Reynolds number based on the airfoil chord increased from about 4.6 million to 8 million with the increase of Mach number. The angle of attack was varied through a range giving normal-force coefficients from near -0.2 to the maximum that could be obtained within the strength limits of each model.

Reduction of Data

Static calibrations of each pair of pressure cells and of the summing circuit were made before and after each run. The sensitivity of each cell was individually adjusted so that its output was proportional to the percentage of the airfoil chord represented by that cell.

The intensity of the normal-force fluctuations was taken as one-half the average of the three largest measurements of peak-to-peak height on the sum trace.[2] Oscillograph records for each Mach number and angle-of-attack setting had an average duration of about one second. Figure 4 illustrates the method of measuring peak-to-peak heights. The intensities of the pitching-moment fluctuations were taken as the rms deviations from the mean of the summation of the instantaneous moments about the 25-percent-chord line indicated by the trace for each cell. Measurements were made of instantaneous deflections of each trace at 1/480-second intervals in order to calculate these rms displacements.

For each Mach number and angle-of-attack setting, a photographic record was taken of the indicated static pressures on the airfoils which were measured by mercury-in-glass manometers. The static normal-force coefficient was computed from these static-pressure measurements.

The test data have been reduced to standard NACA coefficient form. The Mach numbers were corrected for constriction effects by the methods of reference 6; the force and moment coefficients were not corrected. No corrections were applied for wall boundary-layer effects on the buffeting forces. Since examination of spanwise pressures measured on three models at the 75-percent-chord stations and at distances up to 30 percent of the chord on either side of the midspans showed essentially

---

[2]From a limited number of rms intensities of Δc_n computed for six of the airfoils, it appeared that trends were the same as those obtained by peak-to-peak measurements.

a flat distribution, it is believed that any effects of the walls on the trends shown were small.

RESULTS AND DISCUSSION

The results of this investigation are presented, first, to consider the types of pressure pulsations which may be associated with buffeting and, second, to show the normal-force and pitching-moment fluctuations which result from these pulsations. The basic data are given, followed by contours of constant-intensity fluctuations for the individual airfoils to present the normal-force fluctuations. In addition, fluctuation intensities for all the airfoils are shown together for constant Mach numbers so that an over-all comparison of the results can be made.
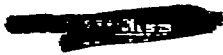
Since the fluctuations of pitching moment computed from a limited number of data appear small, major emphasis has been placed on the normal-force results. The intensities of pitching-moment fluctuations which were measured, however, are shown for all the airfoils at constant Mach numbers so that, as with the normal force, an over-all picture of the results can be obtained.

Types of Pulsations Which May be Associated With Buffeting

Oscillograph records have been examined and two main types of pressure pulsations have been observed. Portions of records which illustrate these types are shown in figure 4; static-pressure distributions corresponding to these sample records are shown in figure 5.

A record for the model with the NACA $65_{(06)}A004$ section is given to show the nature of the pulsations arising from an intermittent build-up and dropping of the pressure peak near the leading edge (fig. 4(a)). Upon consideration of the proportionality factor of the cell sensitivities, it is apparent that the largest pulsations occurred at the pressure-cell station closest to the leading edge. The pulsations were of decreasing intensity along the chord in the region where the pressure was rising rapidly on the upper surface, back to approximately 45-percent chord. Although evidence available at present is not completely conclusive, it is believed that these pressure pulsations near the leading edge are associated with leading-edge separation.

The other record (fig. 4(b)), shown for the NACA 65A012 profile, illustrates the type of pulsations attributable to shock-wave motion and unsteady air flow following the shock wave. In this case the pulsation level near the leading edge was small. The high pulsation level at 45-percent chord, which is just ahead of the rapid pressure

rise shown in figure 5, indicates that the shock wave, along with the corresponding location of the pressure rise through the shock wave, was fluctuating back and forth across the 45-percent-chord station. Pulsations of considerably lesser intensity occurred on the remainder of the airfoil chord in the region of the pressure recovery following the shock wave.

Normal-Force Fluctuations

Basic data.- The basic data, Δc_n, from the sum trace are given in figure 6 as a function of normal-force coefficient for various Mach numbers for the two-dimensional models. Normal-force coefficients were calculated from the measurements of static pressure on the airfoil surfaces.

Contours of constant Δc_n for individual airfoils.- Figure 7 shows contours of constant intensity of normal-force fluctuations as a function of Mach number and normal-force coefficient for each of the models. The plots are arranged so that a variation of thickness ratio is represented in the vertical direction and a variation of thickness distribution in the horizontal direction. From figure 7 it can be noted that, for the 65A-series airfoils at the lower Mach numbers, the contours tend to change position from higher to lower normal-force coefficients as thickness is reduced, a result which can be attributed to an increase in the pressure pulsations near the leading edge. At the higher Mach numbers, however, the contours tend to occur at higher normal-force coefficients with decrease in thickness. This is believed to be due to a decrease in the effects of shock-wave motion and the unsteady flow following the shock wave. The $65_{(06)}A002$ model shows an exception to the above trends at the higher speeds in that the contours generally occur at lower normal-force coefficients than for the $65_{(06)}A004$ airfoil, which indicates that there is a limit to the beneficial effects which a reduction of thickness has on buffeting forces. As the section profiles were changed from those of the 65A series, similar changes in the positions of the contours took place. For the 8-percent-thick airfoils, the general effect of a forward movement of the position of maximum thickness (NACA 2-008) appears similar to an increase in thickness, while the effect of a rearward movement (NACA 877A008) appears somewhat similar to a reduction of thickness, particularly at the lower Mach numbers. It can be seen that the favorable high lift characteristics of the NACA 2-008 airfoil at low speeds are reflected in the high normal-force coefficients at which the fluctuation intensities are reached at lower speeds.

For the 4-percent-thick airfoils it appears that the main difference in the shapes of the contours occurs at the higher Mach numbers in the region of the lower intensity fluctuations where the contours for the

circular-arc airfoil extend to lower normal-force coefficients. In general, for the higher fluctuation intensities, however, the differences between the contours for the two airfoils appear small.

An indication of the rate of increase of the normal-force fluctuations as the normal-force coefficient was increased for each of the airfoils can be seen from the spacing of the contours in figure 7. Normally, it appears that the intensity increase was not particularly abrupt for any of the airfoils in the region below maximum lift. It should be noted that the 65A012 was the only airfoil investigated which reached maximum lift (Mach numbers 0.5 to 0.64 in the region of the ±0.030 contour).

Comparison of Δc_n intensities for all airfoils.- Figure 8 shows the intensities of Δc_n for all the airfoils as functions of normal-force coefficient. The data are presented in the same form as the basic data (fig. 6), but have been cross-plotted as functions of Mach number and replotted in this form at common Mach numbers for all the airfoils. From figure 8 it can be seen that any one airfoil cannot be selected as having the most favorable characteristics over the entire range of these data. At the lower speeds, the thinner airfoils having the sharper leading edges suffered higher intensities (attributable to pressure pulsations near the leading edge). On the other hand, those airfoils generally showing the lower intensities for a given normal-force coefficient at low speeds had poorer characteristics at higher Mach numbers. For Mach numbers below 0.6, figure 8 shows that either the NACA 65A012 or the NACA 2-008 airfoil had the lowest fluctuations for a given normal force. For Mach numbers of 0.75 and above, the NACA $65_{(06)}A004$ airfoil showed the lowest fluctuations. Judging from the trends shown, it appears that by moving the position of maximum thickness forward and by using a larger leading-edge radius than that of the $65_{(06)}A004$ airfoil, an improvement might be made in the low-speed characteristics of this airfoil with only a small sacrifice at the higher speeds.

Pitching-Moment Fluctuations

In order to determine the intensities of the fluctuations of pitching moment, a limited number of data have been analyzed. From these data figure 9 has been prepared which shows curves of Δc_m as a function of normal-force coefficient for various Mach numbers. It can be seen that, in general, the pitching-moment fluctuations were small. It also appears that the obvious trends indicated by figure 9 are similar to those indicated by the lift-fluctuation data in figure 8. It has been concluded, therefore, that within this range of data, fluctuations of pitching moment would not be a principal consideration in the selection of an airfoil section.

CONCLUSIONS

From an investigation of buffeting-force characteristics of seven symmetrical two-dimensional airfoils conducted through a Mach number range of about 0.4 to 0.9 (corresponding Reynolds number range, 4.6 million to 8 million) the following conclusions can be drawn:

1. There appear to be two principal types of pressure pulsations associated with buffeting forces: pulsations which arise from an intermittent build-up and dropping of the pressure peak near the leading edge, and pulsations which are attributable to shock-wave motion and unsteady air flow following the shock wave.

2. No one of the seven airfoils tested has the lowest normal-force fluctuations over the entire range of Mach numbers and normal-force coefficients investigated. For Mach numbers below 0.6, fluctuation intensities were lowest on either the NACA 65A012 or the NACA 2-008 airfoils, but for Mach numbers of 0.75 and above, the intensities were generally lowest on the NACA $65_{(06)}A004$ airfoil.

3. There may be a limit to the beneficial effects which a reduction of thickness has on buffeting since, for symmetrical 65A-series airfoils, a 2-percent-thick airfoil had buffeting forces which were more severe than those on a 4-percent-thick airfoil.

4. An improvement might be made in the low-speed buffeting-force characteristics of the NACA $65_{(06)}A004$ airfoil with only a small sacrifice in its superior characteristics at the higher speeds by moving the position of maximum thickness forward and by using a larger leading-edge radius than that of the $65_{(06)}A004$ airfoil.

5. Fluctuations of pitching moment appear small, and would probably have little influence on the selection of an airfoil for most purposes.

Ames Aeronautical Laboratory
    National Advisory Committee for Aeronautics
        Moffett Field, Calif., Nov. 24, 1953

REFERENCES

1. Humphreys, Milton D.: Pressure Pulsations on Rigid Airfoils at Transonic Speeds. NACA RM L51I12, 1951.

2. Humphreys, Milton D., and Kent, John D.: The Effects of Camber and
       Leading-Edge-Flap Deflection on the Pressure Pulsations on Thin
       Rigid Airfoils at Transonic Speeds. NACA RM L52G22, 1952.

3. Sorenson, Robert M., Wyss, John A., and Kyle, James C.: Preliminary
       Investigation of the Pressure Fluctuations in the Wakes of Two-
       Dimensional Wings at Low Angles of Attack. NACA RM A51G10, 1951.

4. Graham, Donald J.: The Development of Cambered Airfoil Sections
       Having Favorable Lift Characteristics at Supercritical Mach
       Numbers. NACA Rep. 947, 1949.

5. Erickson, Albert L., and Robinson, Robert C.: Some Preliminary
       Results in the Determination of Aerodynamic Derivatives of Control
       Surfaces in the Transonic Speed Range by Means of a Flush-Type
       Electrical Pressure Cell. NACA RM A8H03, 1948.

6. Allen, H. Julian, and Vincenti, Walter G.: Wall Interference in a
       Two-Dimensional-Flow Wind Tunnel, with Consideration of the Effect
       of Compressibility. NACA Rep. 782, 1944.
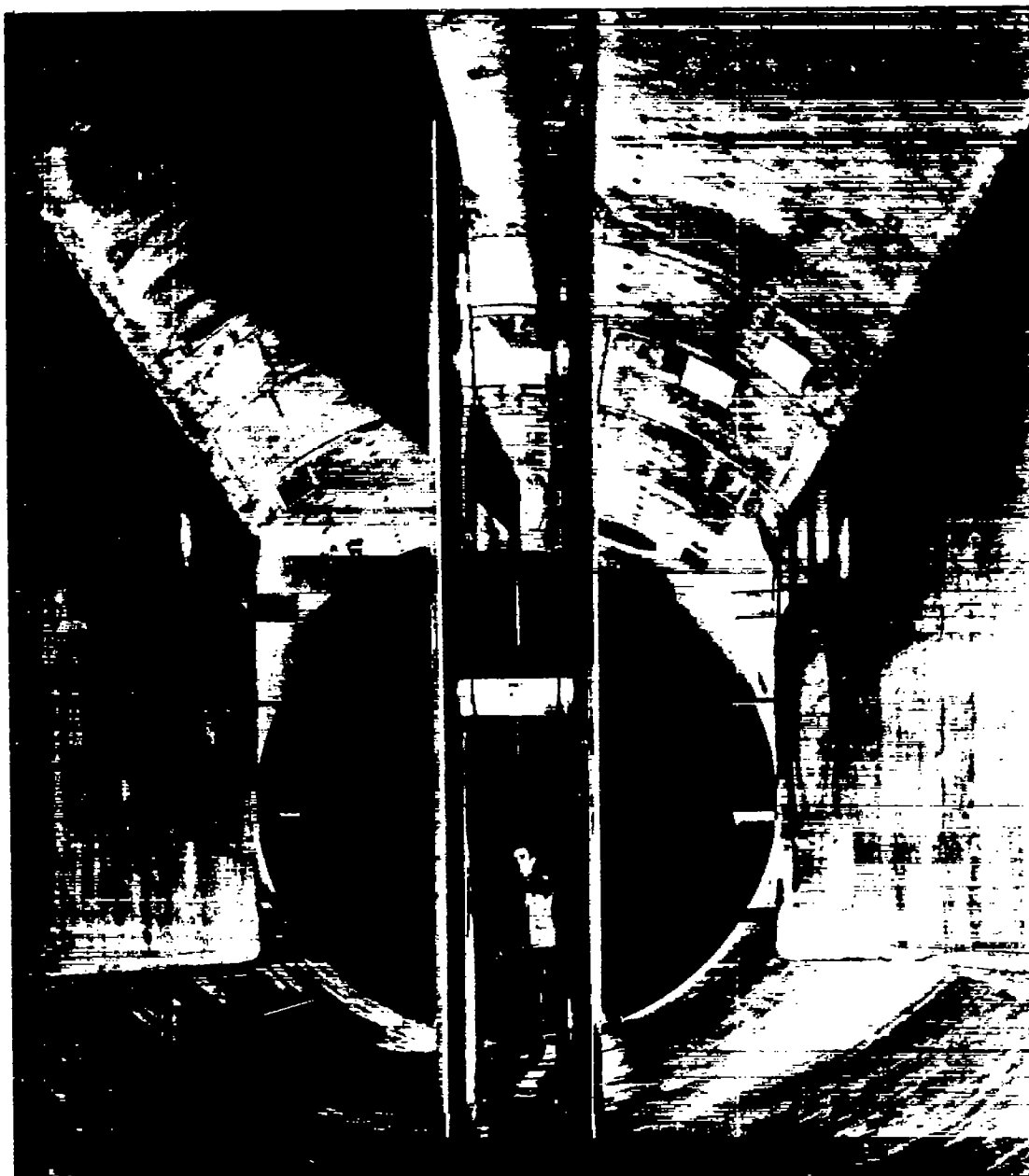
A-14566

Figure 1.- View of the two-dimensional channel in the 16-foot high-
speed wind tunnel showing a model mounted between the walls.

NACA 65A012

NACA 2-008

NACA 65A008

NACA 877A008

NACA 65(06)A004

4% circular arc

NACA 65(06)A002
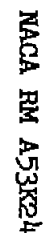
Figure 2.- Section profiles of the models investigated.
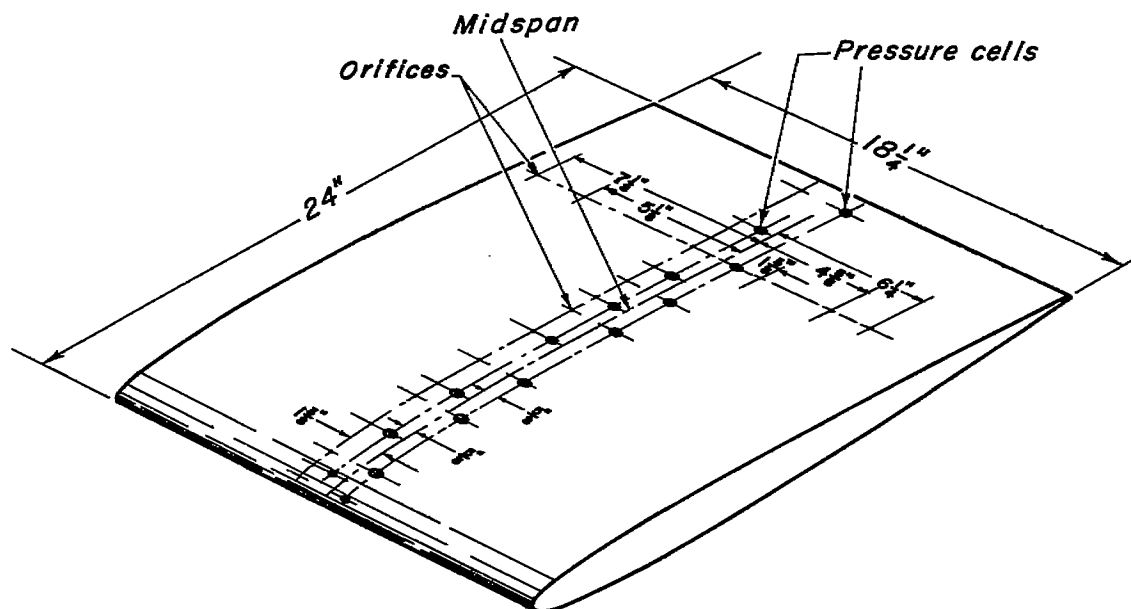
MODEL PRESSURE-CELL AND ORIFICE LOCATIONS
[In Percent of Model Chord]

Cell and orifice number	65A012 and 65A008	65(06)A004 2-008 877A008	65(06)A002	4-percent circular arc
1	1.25	1.25	5	5
2	3.75	3.75	15	10
3	7.5	7.5	25	15
4	15	15	35	22.5
5	22.5	22.5	45	27.5
6	27.5	27.5	55	35
7	35	35	65	45
8	45	45	75	52.5
9	52.5	52.5	85	57.5
10	57.5	57.5		62.5
11	62.5	62.5		67.5
12	67.5	67.5		75
13	75	75		85
14	85	85		90
15	95	90		95

Figure 3.- Sketch of a typical model with a table of the pressure-
cell and orifice locations for all the models.

Percent
chord

Oscillograph 2

1.25
3.75
7.50

15.00

←.01 Sec

22.50
27.50

35.00

45.00

52.50
57.50

62.50
67.50

Oscillograph 1

75.00

85.00

90.00

Peak-to-peak
heights

Sum

65(06)A004
Section
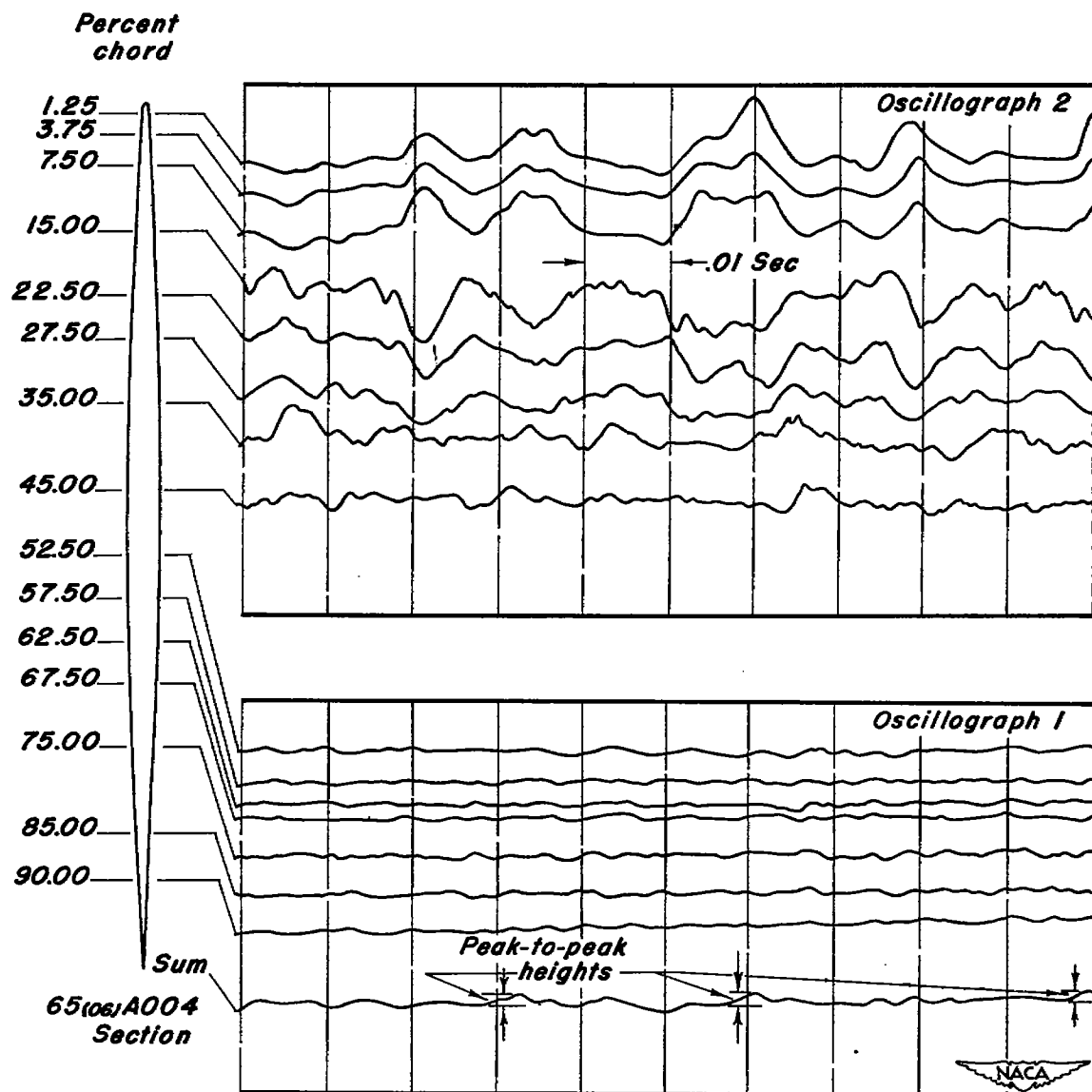
NACA

(a) NACA 65(06)A004; M, 0.59; C_n, 0.61.

Figure 4.- Sample oscillograph records.
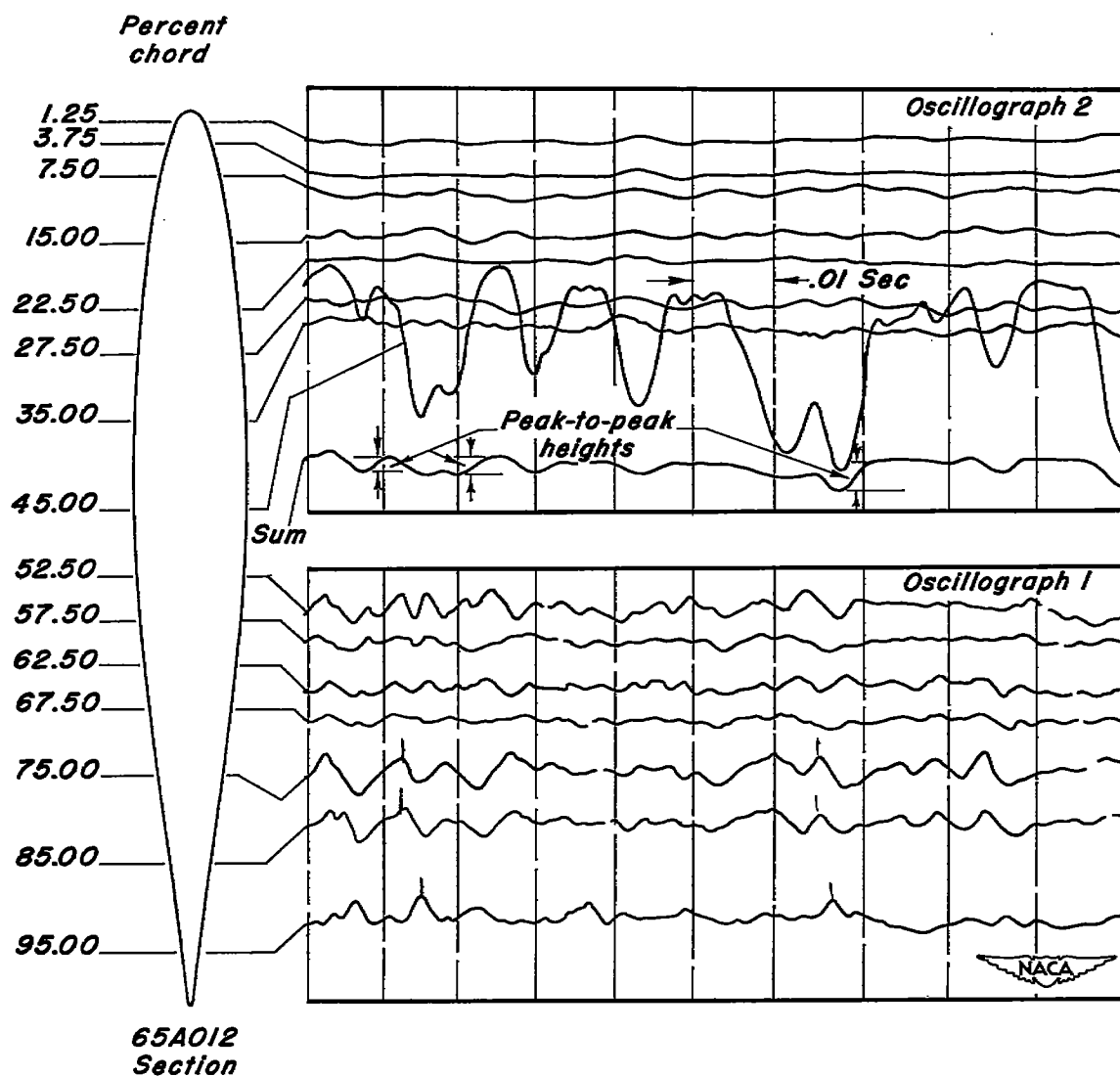
(b) NACA 65A012; M, 0.79; C_n, 0.47.

Figure 4.—Concluded.
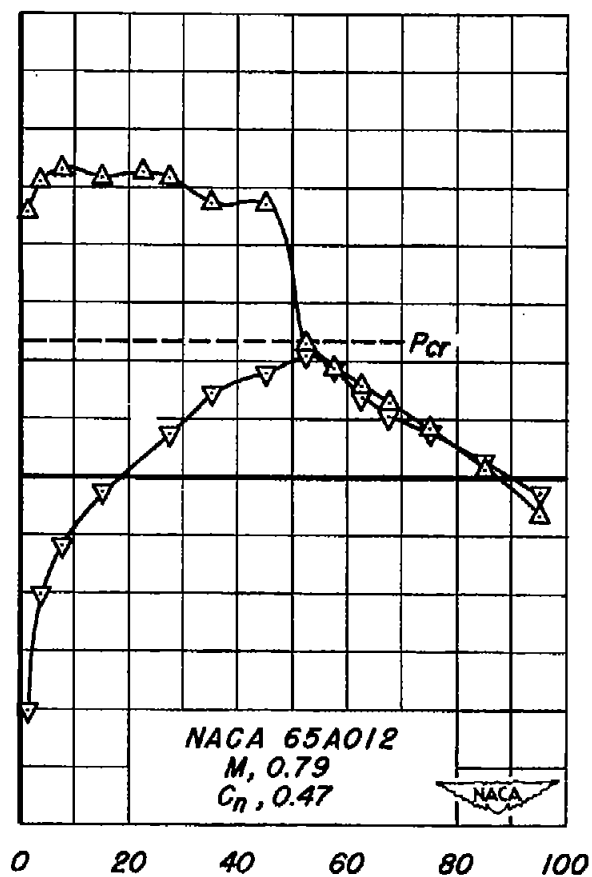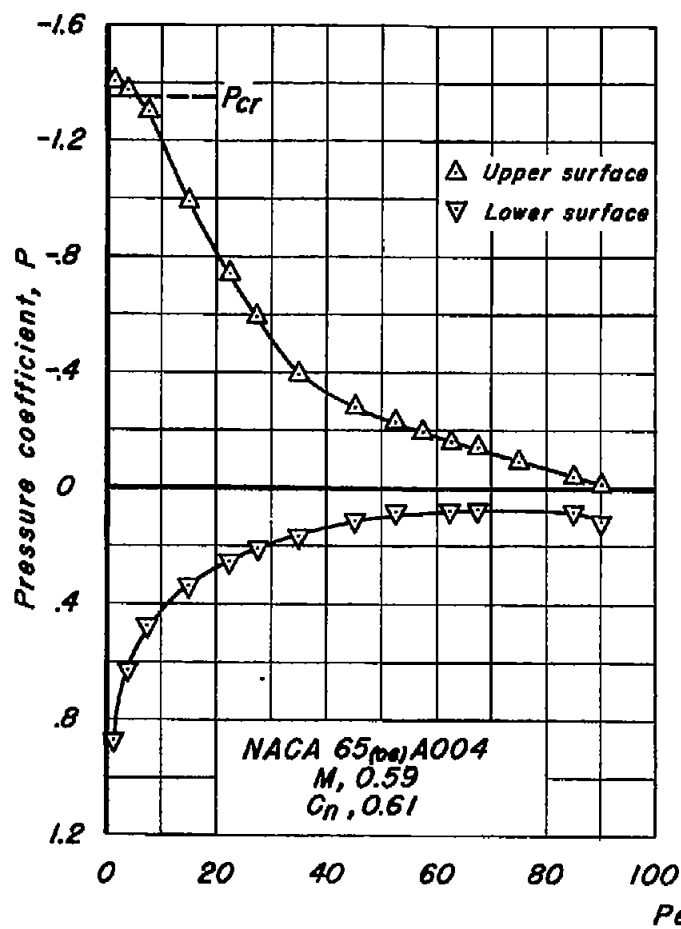
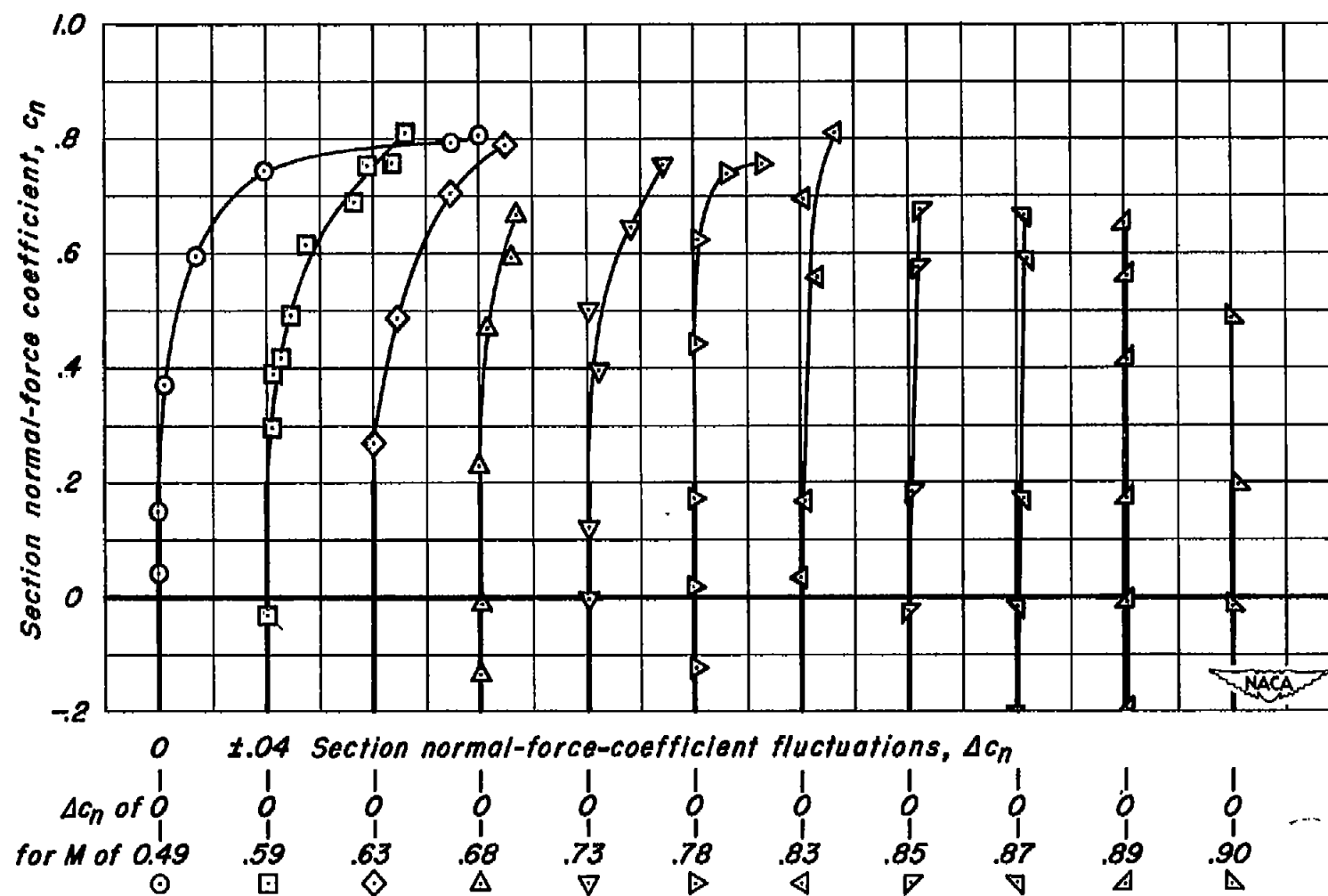Figure 5.- Static-pressure distributions on the models corresponding to the sample records.
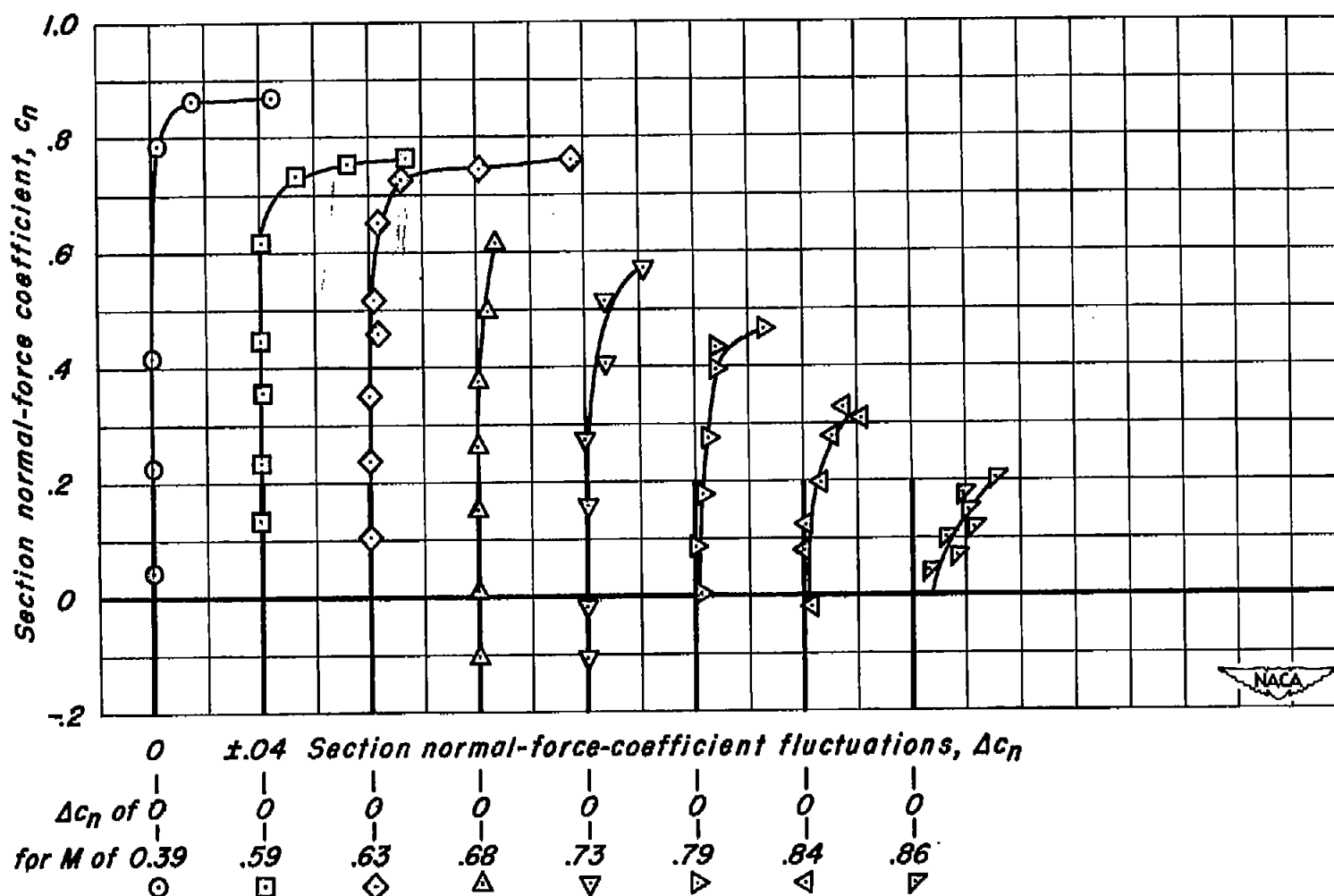
(a) NACA 65A012.

Figure 6.- The intensity of section normal-force-coefficient fluctuations as a function of section normal-force coefficient.
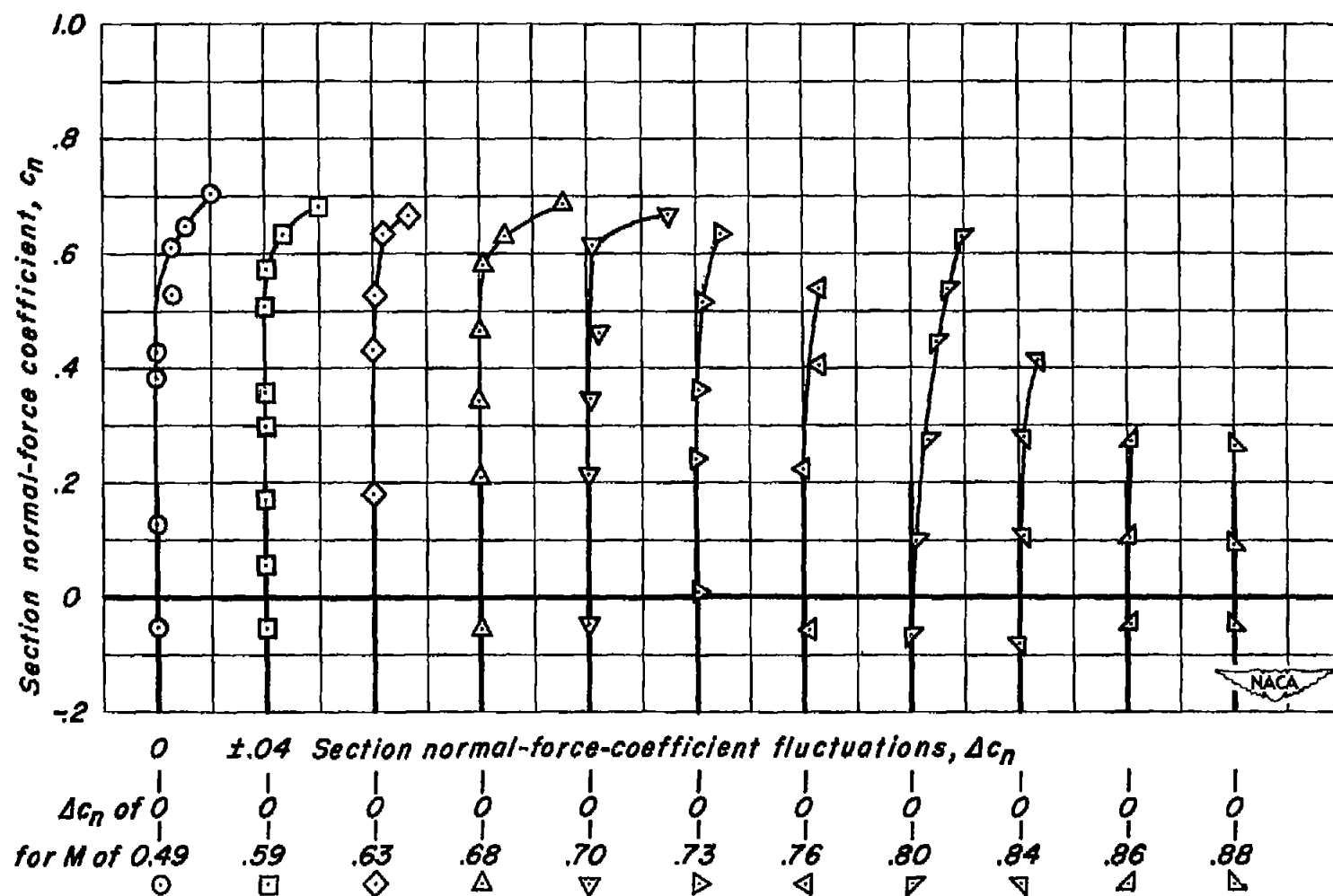
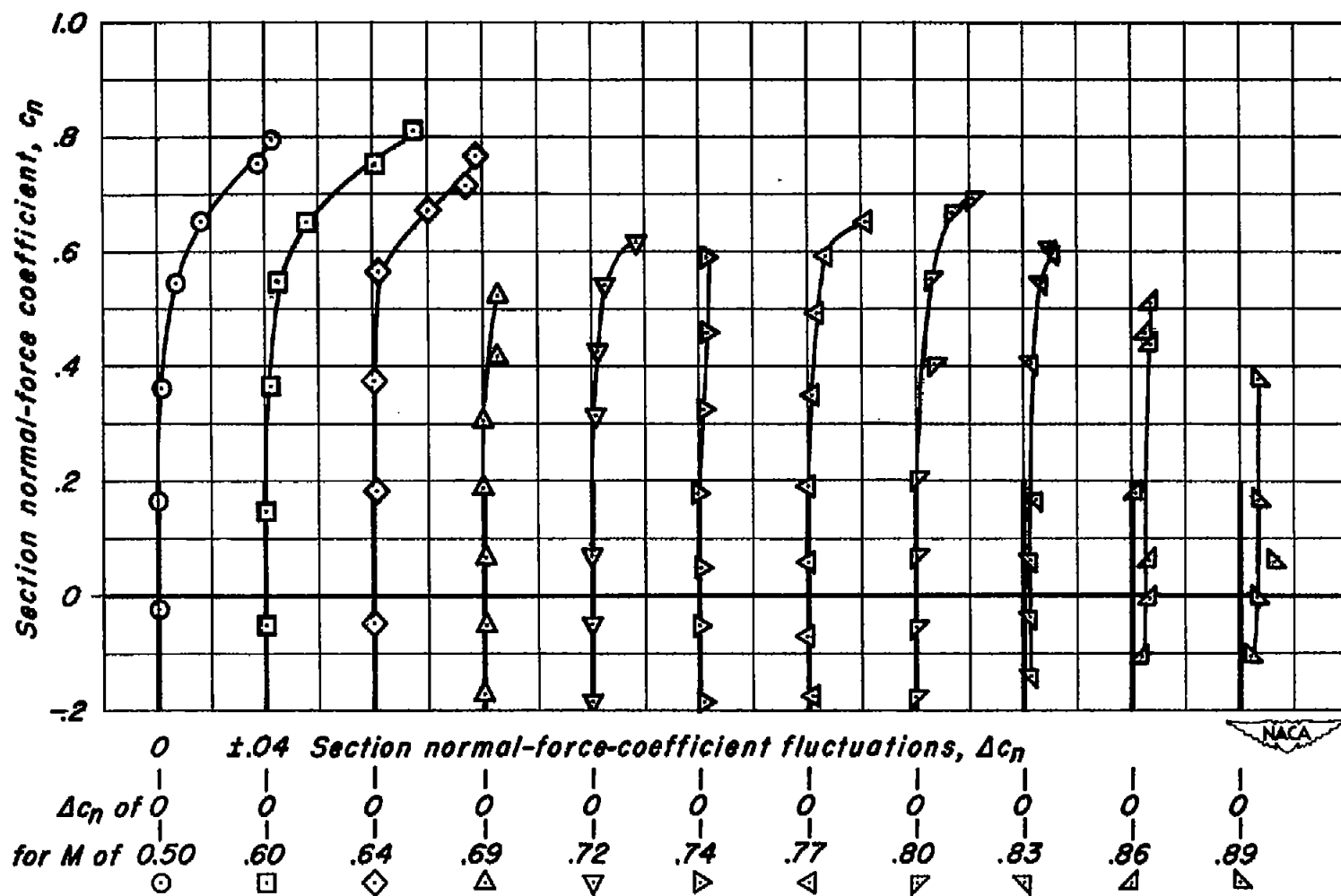(b) NACA 65A008.

Figure 6.- Continued.
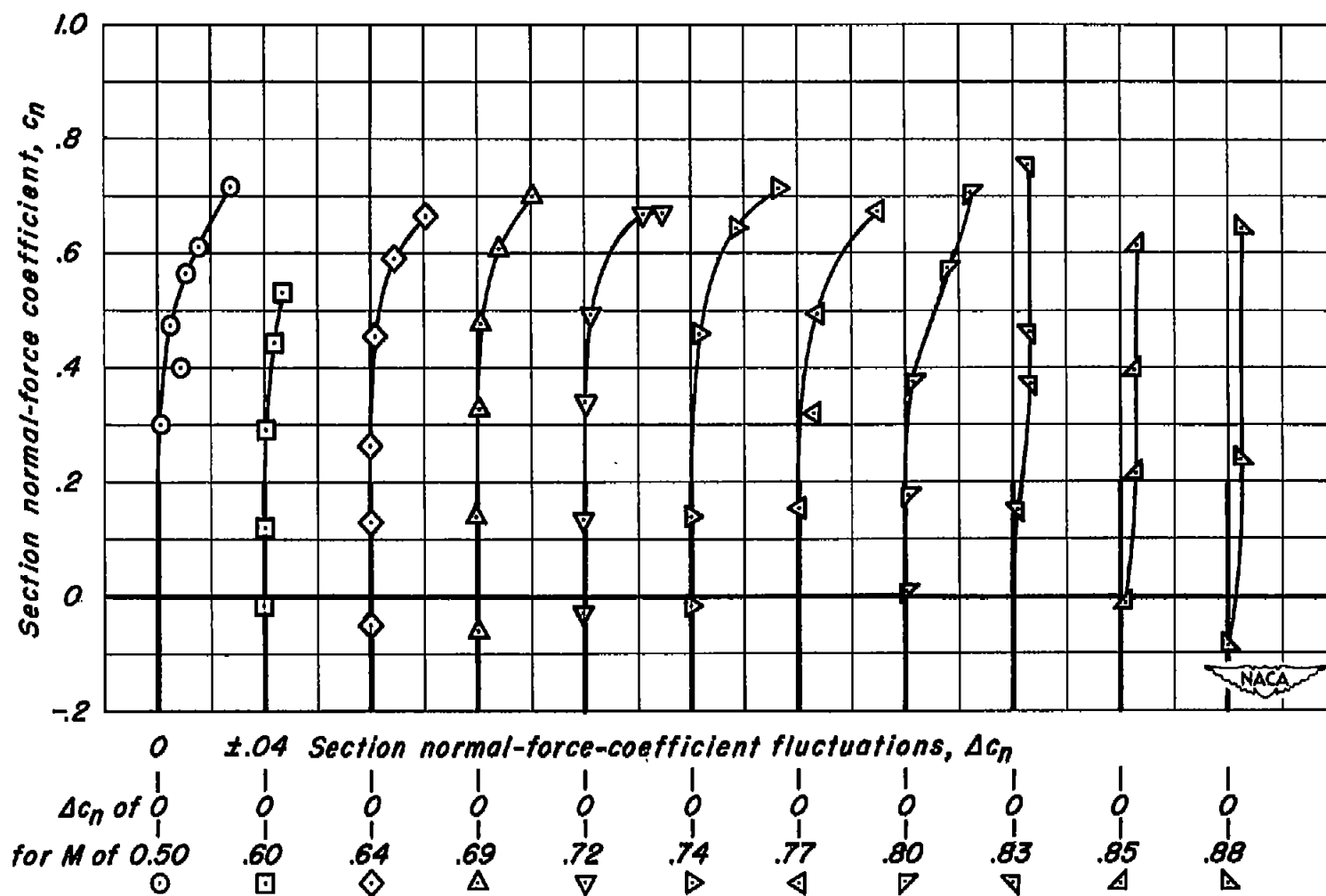
(c) NACA 65(06)A004.

Figure 6.- Continued.
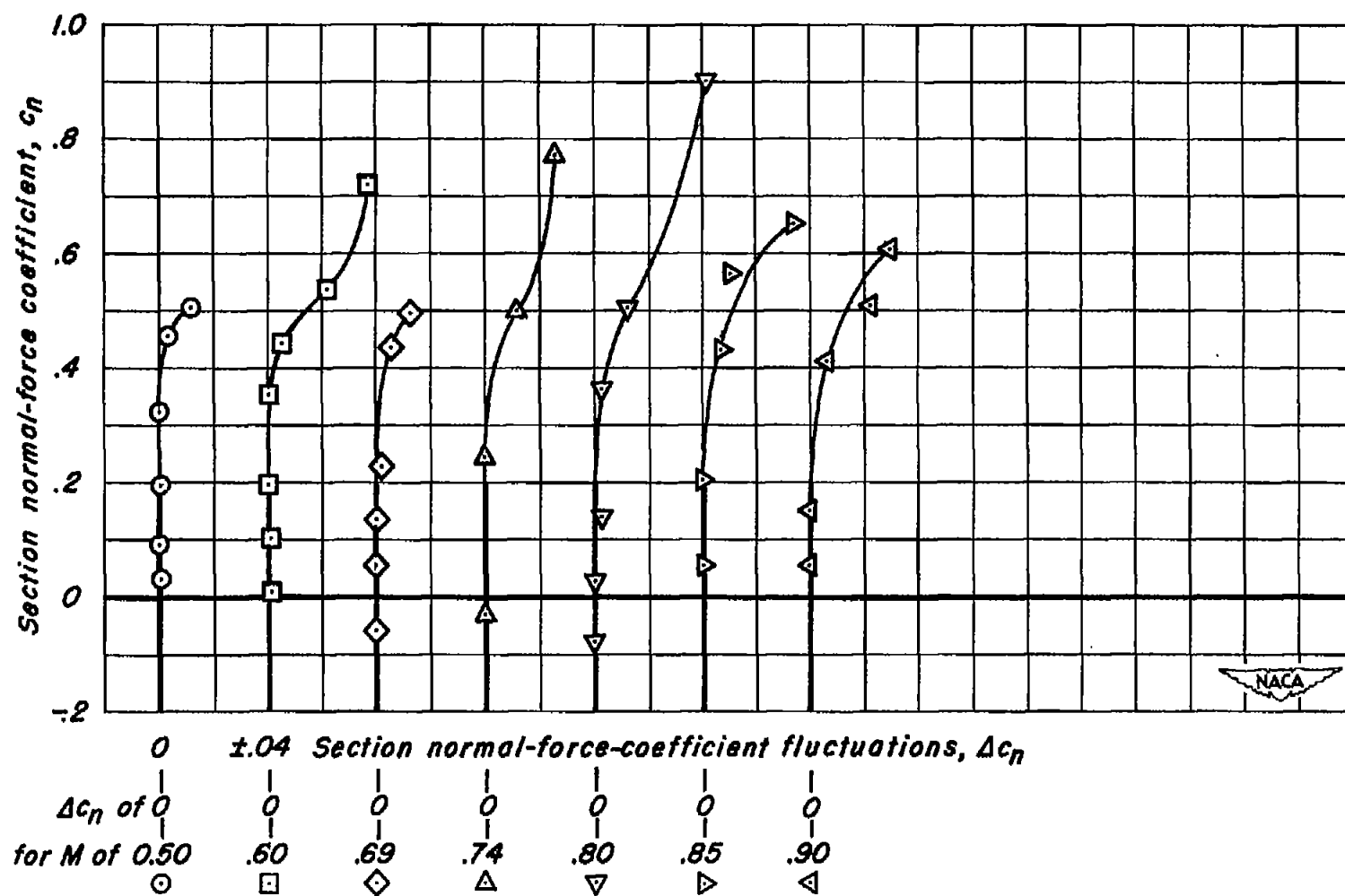
(d) NACA 65(06)A002.

Figure 6.- Continued.

(e) NACA 2-008.
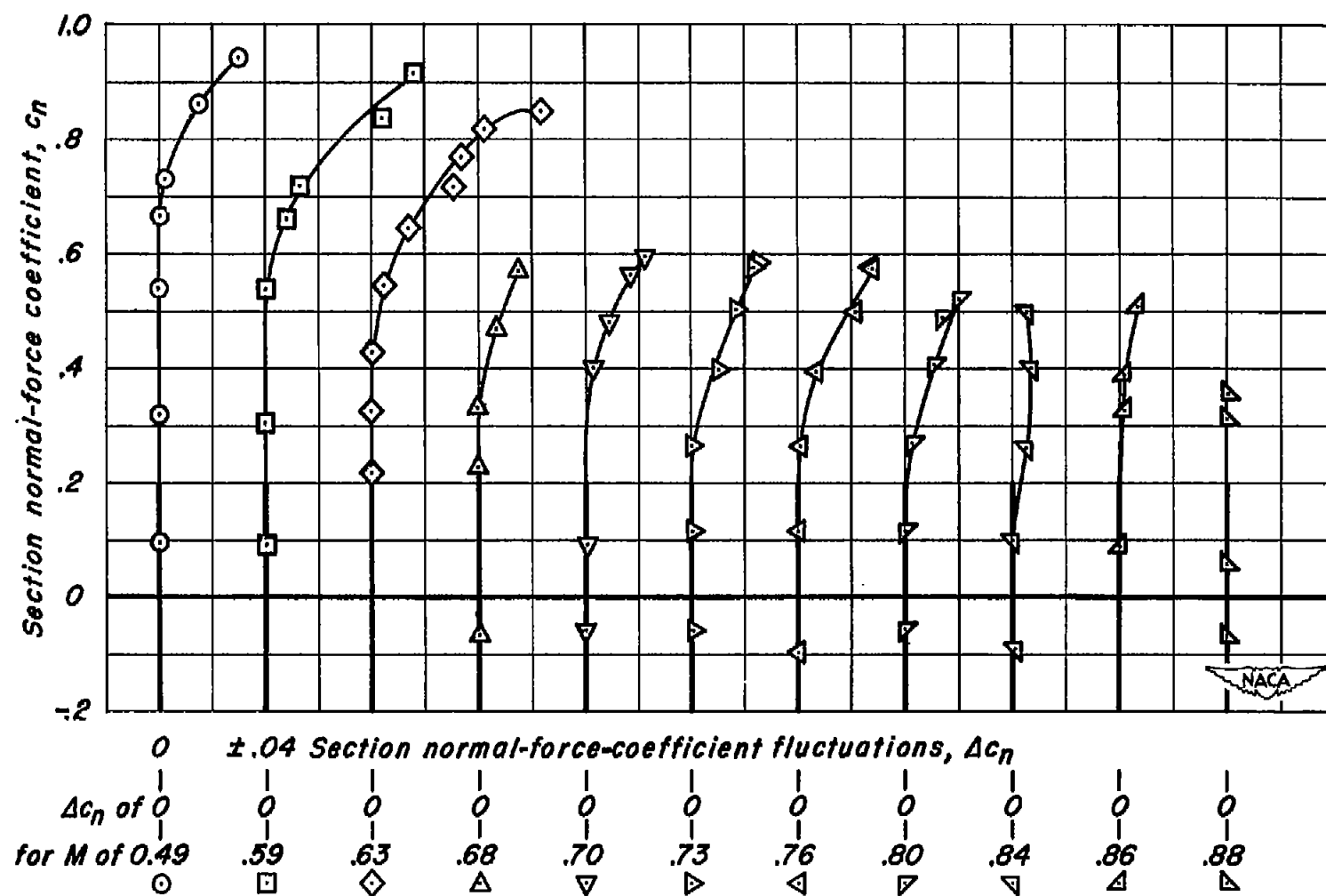
Figure 6.- Continued.

(f) NACA 877A008.

Figure 6.- Continued.

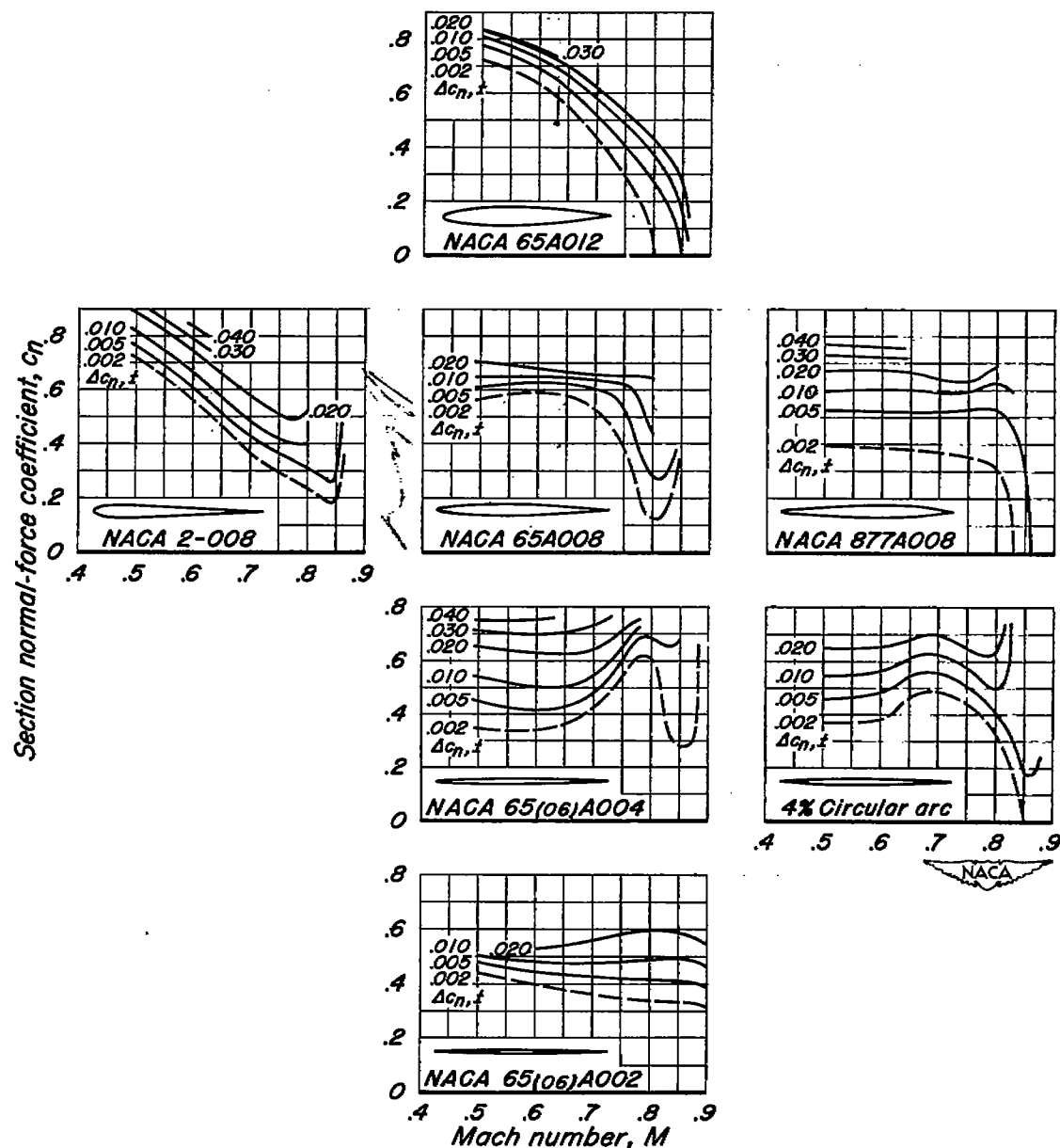(g)   4-Percent circular arc.

Figure 6.- Concluded.

CONFIDENTIAL

Figure 7.- Contours of constant intensity of normal-force-coefficient
fluctuations as a function of Mach number and normal-force
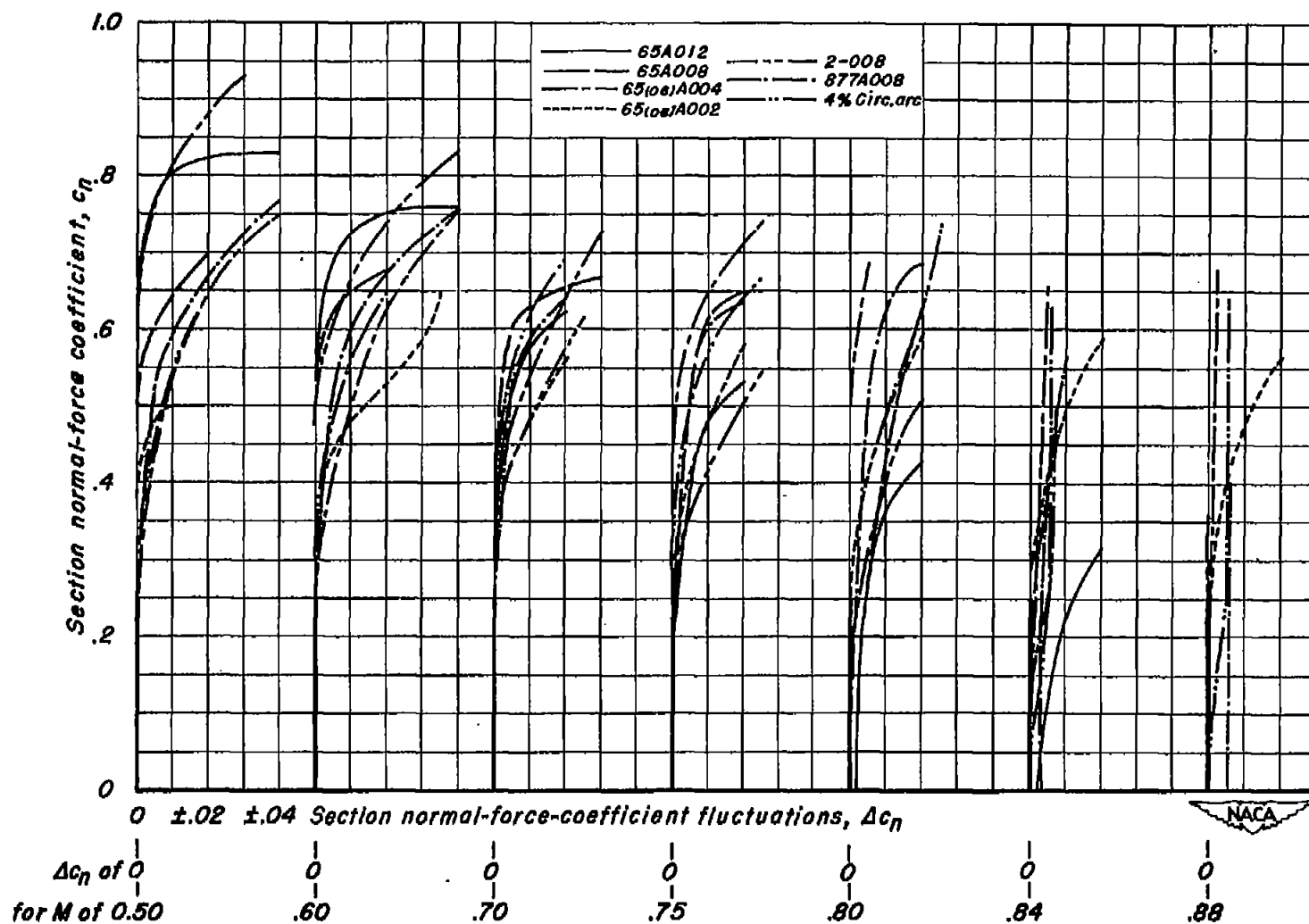coefficient.

CONFIDENTIAL

Figure 8.- A comparison of the intensities of section normal-force-coefficient fluctuations for all the models as a function of section normal-force coefficient.
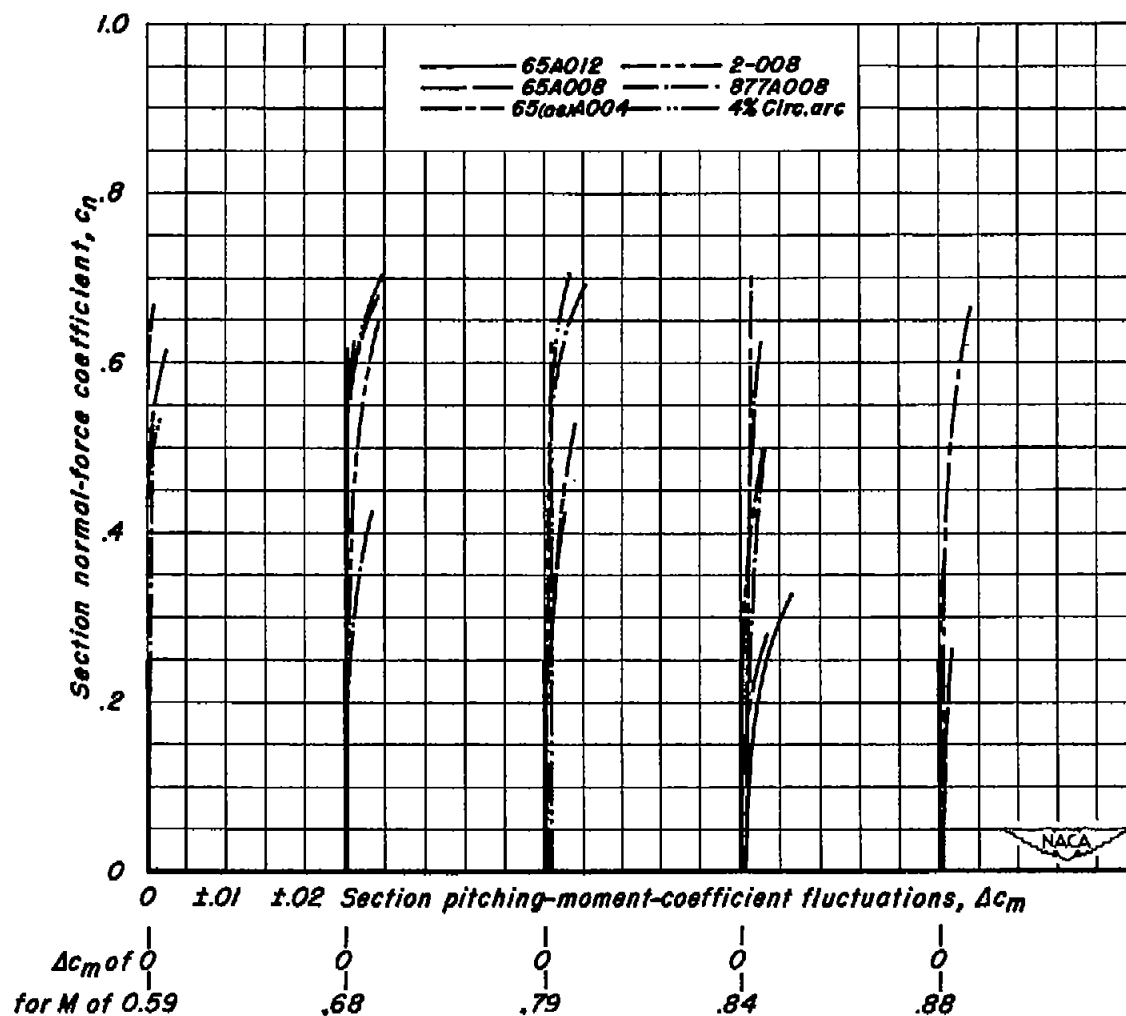
Figure 9.- A comparison of the intensities of section pitching-moment-coeffi-
cient fluctuations for six airfoils as a function of section normal-force
coefficient.

3 1176 01434 7919